Metabolomics reveals that chronic restraint stress alleviates carbon tetrachloride-induced hepatic fibrosis through the INSR/PI3K/AKT/AMPK pathway

Shanshan Zhang
Guangzhou University of Chinese Medicine
Binjie Liu
Guangzhou University of Chinese Medicine
Lan Huang
Guangzhou University of Chinese Medicine
Rong Zhang
Guangzhou University of Chinese Medicine
Lin An (anlin@gzucm.edu.cn)
Guangzhou University of Chinese Medicine https://orcid.org/0000-0003-1678-421X
Zhongqiu Liu
Guangzhou University of Chinese Medicine

Research Article

Keywords: hepatic fibrosis, chronic restraint stress, metabolomics, INSR pathway, carbon tetrachloride

Posted Date: May 30th, 2023

DOI: https://doi.org/10.21203/rs.3.rs-2536417/v1

Version of Record: A version of this preprint was published at Journal of Molecular Medicine on November 23rd, 2023. See the published version at https://doi.org/10.1007/s00109-023-02395-4.

Abstract

Hepatic fibrosis (HF) could be developed into liver cirrhosis or even hepatocellular carcinoma. Stress has an important role in the occurrence and development of various considerable diseases. However, the effect of a certain degree stress on HF is still controversial. In our study, stress was simulated with regular chronic restraint stress (CRS) and HF model was induced with CCl_4 in mice. We found that CRS was able to attenuate CCl_4-induced liver injury and fibrosis in mice. Surprisingly, behavioral analysis showed that the mice in the HF group exhibited depression-like behavior. Further, the metabolomic analysis revealed that 119 metabolites and 20 metabolic pathways were altered in mice liver, especially the betaine metabolism pathway. Combined with the results of ingenuity Pathway Analysis (IPA) analysis, the key proteins INSR, PI3K, AKT, and p-AMPK were identified and verified, and the results showed that CRS could upregulate the protein levels and mRNA expression of INSR, PI3K, AKT, and p-AMPK in liver tissues of HF mice. It suggested that CRS alleviated CCl_4-induced liver fibrosis in mice through upregulation of the INSR/PI3K/AKT/AMPK pathway. Proper stress might be a potential therapeutic strategy for the treatment of chronic liver disease, which provided new insights into the treatment of HF.

1 Introduction

Hepatic fibrosis (HF) caused by various chronic stimuli, such as viruses, alcohol, and autoimmune diseases, which is characterized by excessive deposition of extracellular matrix (ECM), is a reversible pathological process[1–2]. Hepatic stellate cells (HSCs) play a significant role in the development of HF, activated HSCs are the key effectors of fibrogenesis. They are activated and transformed into myofibroblasts when damaged by pathogenic factors and participate in the injury repair process[3–4]. The nature of HF is a wound healing response, but without appropriate intervention, it can progress to cirrhosis, portal hypertension, and hepatocellular carcinoma, resulting in increased morbidity and mortality[5]. However, there are still no approved antifibrotic therapies for liver disease. Thus, there is an exigent need to clarify the cellular and molecular mechanisms of fibrosis regression in order for treating liver disease[6].

Stress is used to refer to a condition where various or perceived stimuli alter the homeostatic state of an organism[7], which regular accompanies with patients and exists in the process of disease therapy. Stress has an important role in the occurrence and development of various consider able diseases among cardiovascular[8], digestive[9], immune[10], and nervous system[11].A number of early reports have suggested that stress serves a major role in the initiation, course and outcome of liver diseases. Study demonstrated that chronic restraint stress (CRS) decreased the repair potential from mesenchymal stem cells on liver injury by inhibiting TGF-β1 generation, thereby reducing HF[12]. Another work showed that CRS reduces the development of liver fibrosis by inhibiting the activation of hepatic stellate cells via 5-HT2B receptor[13]. In addition, it is reported that stress can attenuate hepatic lipid accumulation via elevation of hepatic β-muricholic acid levels in mice with nonalcoholic steatohepatitis[14]. On the contrary, a few studies demonstrated that stress promoted the progression of liver fibrosis in rats or led to

steatosis and non-alcoholic steatohepatitis[15, 16]. Therefore, the effects of stress on liver disease, especially HF, are widely controversial and uncertain, and the mechanisms remain to be elucidated.

The term "restraint stress" refers to a specific type of stress resulting from the restriction of movement. In our study, we constructed an animal model by giving restraint stress while inducing liver fibrosis in mice with CCl_4. We attempted to elucidate the effect of CRS on liver fibrosis and the potential signaling pathways. The workflow of this study was summarized in Fig. 1.

2 Methods and Materials

2.1 Chemicals and reagents

The standards of reserpine and cholic acid-d4 were purchased from Sigma Aldrich (St. Louis, MO, USA), betaine (97%) was purchased from TCI (Shanghai, China). HPLC grade acetonitrile was purchased from Merck & Co (Billerica, MA, USA). Ultrapure water was produced from a Milli-Q system (Millipore, MA, USA). The alanine transaminase (ALT), aspartate aminotransferase (AST), alkaline phosphatase (ALP), and hydroxyproline detection kits were acquired from Nanjing Jiancheng Bioengineering Institute (Nanjing, China).

2.2 Animals experiments

Male C57BL/6 mice aged 6–8 weeks were obtained from the Guangzhou Baiyun District Suibei Experimental Animal Farm (Guangzhou, China). The mice were maintained under controlled conditions (22 ± 2 ℃, 60% ± 5% humidity, 12 h/12 h day/night cycle) and given standard water or food ad libitum. The animal experiments were approved by the Institutional Animal Care and Use Committee of Guangzhou University of Traditional Chinese Medicine (reference No. 20211102).

The mice were randomly divided into four groups: (1) control group: given olive oil; (2) CRS group: given CRS procedure; (3) HF group: given CCl_4; (4) HF + CRS group: given CCl_4 and CRS procedure.

Mouse model of HF

to induce a liver fibrosis model, the mice were injected intraperitoneally with 15% CCl_4 (v/v, dissolved in olive oil) at a concentration of 5.0 mL/kg twice a week for 9 weeks continuously.

CRS procedure

the mice were assigned to restraint tubes (50 mL conical tubes) and restrained for 4 hours per day for 9 weeks. In the tubes, they could not move freely and did not have access to water or food, but they were not pressed and could breathe freely.

2.3 Evaluation of liver function and fibrosis

Liver function analysis

Serum of mice was collected by centrifugation at 3000 rpm, 4°C for 10 min. The serum levels of the ALT, AST, and ALP were measured by commercially available kit.

Hematoxylin and eosin staining

Liver tissues were fixed in 4% formaldehyde solution and then embedded in paraffin. Afterwards, 4 μm thick sections were cut by using a RM2016 microtome (Leica, Shanghai, China). stained with hematoxylin-eosin (H&E).

Fibrotic test

To detect liver fibrosis, the paraffin sections were stained with Masson's Trichrome Staining, the blue-stained areas in the tissue sections were assessed using an Image-Pro Plus image analyzer (Media Cybernetics, Inc., Rockville, MD, USA) for semi-quantitative analysis. Hydroxyproline levels in mice serum were measured with hydroxyproline detection kit.

2.4 Behavioral studies

Sucrose preference test (SPT)

Animals were first trained to consume a 1% sucrose solution from two differing bottles (48 h before the formal experiment). Twenty-four hours later, the animals were allowed free access to 1% sucrose and water from two differing bottles. To avoid bottle side preference, the two bottles were switched. The amounts in the two bottles were measured after 24 h and sucrose preference was calculated.

Open field test (OFT)

We characterized mice behavior as they freely explored an open-field plastic chamber (40 cm width × 40 cm length × 30 cm height) using a video tracking system (Smart 3.0). The mice were placed in this arena for 10 min, and time spent in the center region during the final 5 min period was recorded.

Tail suspension test (TST)

The mice were suspended by their tails for 6 minutes from a metal rod (30 cm above the ground) and monitored using a video tracking system (Smart 3.0). Immobility duration period was recorded during the final 4 min.

Forced swimming test (FST)

Mice were placed in a container filled with water that eventually resulted in immobility, reflecting behavioral despair. Water (25 ± 1°C) was placed in a transparent acrylic cylinder bath (10 cm in diameter,

30 cm in height) filled to a depth of 15 cm. Mice were placed in the water for six minutes using a video tracking system (Smart 3.0); immobility duration within the final 4 min of testing was recorded.

2.5 Immunohistochemistry and immunofluorescence staining

Immunohistochemistry assay was performed according to method described before[17], α-SMA antibody (Proteintech, 14395-1-AP), collagen type III (N-terminal) polyclonal antibody (Proteintech, 22734-1-AP), and p-AMPKα antibody (Cell Signaling Technology, #2535) were used.

2.6 Metabolomic profiling

Sample preparation: Sample extraction procedure were based on several previous studies with minor modifications[18]. In brief, 50 mg liver tissue was mixed with 200 μL MeOH and the mixtures were vortexed for 3 min, then centrifuged at 14,000 rpm for 15 min at 4°C. Next, the supernatant was vacuum dried, reconstituted in 100 μL of MeOH:H_2O (1:1, v: v) with internal standards (500 nM reserpine and d4-CA) and centrifuged at 14000 rpm for 30 min at 4°C before analysis. Quality control (QC) samples were prepared by pooling and aliquoting sample extracts. The distribution of QC data in principal component analysis (PCA) and the standard deviation (STD) of retention times was used to evaluate data quality.

Chromatography and mass spectrometry conditions: LC-MS nontargeted analysis was performed using 1290 ultra-high-performance liquid chromatograph system (Agilent, California, USA) coupled to 6540 Q-TOF mass spectrometry (Agilent, California, USA), operated in positive and negative ion modes. The MS parameters were set as follows: nozzle voltage was set at 1500 V, capillary voltage at 3500 V, fragmentor voltage at 175 V, nebulizer pressure at 35 psi, sheath gas temperature at 350℃ and gas temperature at 320℃. The flow rate of sheath gas and gas were 11 L/min and 8 L/min, respectively. The analyses were separated with Waters BEH C18 column (150 mm, 2.1 x 1.7 μm) at 50℃ column temperature using constant flow rate of 0.4 mL/min. The LC conditions were as follows: 0.1% formic acid in deionized water (solvent A), and 0.1% formic acid in acetonitrile (solvent B); The gradient elution started with 2% B for 1 min, linearly increased to 100% B within 15 min and keep 100% of solvent B for 3 minutes. Afterwards, the composition was brought back to the initial ratio of 2% B within 1 min, followed by 1 min of re-equilibration.

Data processing and analysis: Raw data in both ionization modes was obtained by Mass Hunter Workstation software (Agilent, USA). The raw data format extracted by Profinder 10.0 (Agilent, USA) for selecting peaks, aligning, and then Mass Profiler Professional 15.0 (Agilent, USA) was used integrating to obtain three-dimensional information about the data of each sample, including all ion characteristics and their RT, m/z, and intensity. The output data was imported into SIMCA-P (version 14.1; Umetrics, Umea, Sweden) to conduct multivariate statistical analysis including the PCA and orthogonal partial least squares discriminate analysis (OPLS-DA) to obtain VIP value respectively of each feature. The features with *p* value below 0.05 and VIP above 1 was considered to be the potential differential metabolites.

Accurate mass data and isotopic distribution for the precursor and product ion were compared to spectral data of the reference compounds in the databases, such as metlin, the Human Metabolome Database (HMDB, https://hmdb.ca/), MassBank (https://massbank.eu/MassBank/), Kyoto Encyclopedia of Genes and Genomes (KEGG, www.genome.jp/kegg/) and our own lab's proprietary database. Finally, the key metabolites were imported into MetaboAnalyst 5.0 (https://www.metaboanalyst.ca/) and Ingenuity Pathway Analysis (IPA, version 1.0, QIAGEN, DUS, Germany) for metabolic pathways analysis and network analysis.

2.7 Western blotting analysis

Liver tissues were homogenized in RIPA buffer, lysed on ice for 40 min, and then centrifuged at 4℃ at 12000 rpm for 10 min. The supernatant was qualified using BCA kit and boiled with loading buffer for 10 min. Thereafter, denatured protein was segregated by SDS polyacrylamide gel electrophoresis, and then transferred onto Immobilon-P-membranes (PVDF membrane). The membranes were blocked by 5% BSA, and then immunoblotted by various primary monoclonal antibodies. The horseradish peroxidase-conjugated goat anti-rabbit secondary antibody and ECL were used to examine the expression of protein. Alpha-SMA antibody (Proteintech, 14395-1-AP), INSR antibody (Proteintech, 20433-1-AP), Phospho-PI3K p85 alpha (Tyr607) Antibody (Affinity, #AF3241), AKT Monoclonal antibody (Proteintech, 60203-2-Ig), p-AMPKα antibody (Cell Signaling Technology, #2535), and AMPKα antibody (Cell Signaling Technology, #2532) were used.

2.8 Real-Time PCR analysis

Total RNA was extracted from liver samples with TRIzol reagent (Accurate Biotechnology Co.,Ltd., Hunan, China) in accordance with the manufacturer's protocol. First-strand cDNA was generated by using 1 μg of total RNA with a SYBR Green I reagent kit (Accurate Biotechnology Co.,Ltd., Hunan, China). The Real-Time PCR reaction was performed on a QuantStudio™ 5 (Applied Biosystems, USA) using QuantStudio™ design and analysis software v.1.5.1. The primers used are listed in Table S1, were purchased from Sangon Biotech (Shanghai, China). Target mRNA was normalized to *Gapdh*. *Gapdh* served as an endogenous control. Relative expression changes were determined using the $2^{-\Delta\Delta Ct}$ method.

2.9 Statistics

All data presented are expressed as arithmetic mean ± *SEM*. All statistical analyses were performed using SPSS software v22.0 (Chicago, IL, USA). For statistical comparisons between two groups, we used Student's T-test or Mann-Whitney U test for normally and non-normally distributed variables to obtain *p* value. For multiple comparisons, we used One-way ANOVA and Bonferroni correction or Kruskal Wallis H test for normally and non-normally distributed variables, respectively. And *p* value below 0.05 was considered statistically significant.

3 Results

3.1 CRS mitigated CCl_4-induced liver injury

We established a CCl_4-induced liver injury model in 6-8-week-old mice. Following 9 weeks exposure of CCl_4, serological and histopathological examinations were performed with appropriate commercial kits. We measured the weekly weight change of the mice during the modeling periods (Fig. 2a), we found that the body weight of mice in the HF, CRS and HF + CRS groups decreased significantly compared with the normal group, but there was no significant difference between the liver fibrosis and HF + CRS group. Long-term and repeated injections of CCl_4 also caused noticeable increase in hepatic index, which indicated edema of the liver. However, compared with the HF group, the liver coefficient of the HF + CRS group instead decreased (Fig. 2b). Furthermore, the pathological observation also showed the same result of liver injury indicated by hepatic index, after CCl_4 induced, the liver was dull and less lustrous, and the liver surface showed obvious diffuse coarse granularity (Fig. 2c). The H&E staining pathological observation clearly showed hepatic morphological lesion with large areas of hepatocyte necrosis and increased inflammatory cells around the hepatic portal and sinusoid in HF (Fig. 2d), which were alleviated by CRS intervention. To further assess the liver function, we measured the serum levels of ALT, AST, and ALP. The results showed that the elevated levels of ALT, AST, and ALP in serum induced by CCl_4, which were diminished in CRS treatment (Fig. 2e). Collectively, all these results indicated that CRS ameliorated CCl_4-induced liver injury.

3.2 CRS attenuated CCl_4-induced HF

To investigate the progression of HF in mice, collagen fiber deposition and HSCs activation hall-marker α-SMA were further measured. Masson's staining showed a significant increase in collagen fiber deposition around periportal areas with marked portal-portal and portal-central bridging in HF group, while it was reduced in the HF + CRS group (Fig. 3a). In addition, the immunohistochemical staining demonstrated α-SMA and type III collagen expression in liver tissues the HF group were remarkedly more than that in HF + CRS group (Fig. 3b, c). Semi-quantitative data was presented for better illustration (Fig. 3d). Also, we examined the protein level of α-SMA and the mRNA expression of α-SMA in mice liver tissue. As shown in Fig. 3e-g, CCl_4 induction enhanced the gene and protein expressions of α-SMA in mice, which were reversed in HF + CRS group. Hydroxyproline is a major component of fibrillar collagen of all types, we also measured the level of hydroxyproline in the serum and the results were consistent with the above (Fig. 3h).

3.3 CCl_4-induced liver fibrosis could cause depression-like behavior

Since CRS is a method of modeling mice depression, we did behavioral tests to determine whether CRS induces depression-like behavior and to observe whether CRS affects the behavior of HF mice in this experiment. Interestingly, experimental results show that mice in the HF group showed the most pronounced depression-like behavior. Compared with the control group, the rate of sucrose preference in the HF group decreased obviously, indicating that the mice in the HF group were deprived of pleasure

(Fig. 4a). Moreover, mice showed a significant increase in immobility duration during TST and FST, indicating that the mice in the HF group were exhibit desperate behavior (Fig. 4b, c). The results of the OFT showed that the central dwell time of mice in the HF groups was reduced compared to the normal group, indicating a reduction in exploratory activity (Fig. 4d, e). Furthermore, the experimental results also showed that compared with the HF group, the TST, SFT and OFT indices of mice in the HF + CRS group did not change much. Surprisingly, the rate of sucrose preference was even improved in the HF + CRS group. This indicated that CRS did not worsen depression-like behavior in HF mice and might even play a positive role in liver fibrosis. By comparing the behavioral results of CRS and the control group, we could find that CRS increased the immobility time of FST and decreased the dwell time in the open field center of mice, while the other two indicators did not change significantly. These data suggested that although CRS had a negative effect on the behavior of normal mice, it has a protective effect on the mice with HF.

3.4 CRS altered metabolomic profiles in HF mice

We performed the metabolomic profiling of mouse liver tissue by using a LC-MS system. QC samples were used to evaluate the technical accuracy and reproducibility of the liver metabolomics profile, PCA scatter plots showed the CV of the QC samples was in the range of ± 3 STD (Fig. S1), indicating good reproducibility of the instrument throughout the batch analysis process. The PCA results (Fig. S2a, b) showed that the four groups could be separated to different degrees in positive and negative ion modes. To highlight the differences, we did OPLS-DA analysis. As shown in Fig. 5a and b, OPLS-DA showed an obvious separation between the Control, CRS, HF, and HF + CRS groups, indicating a difference in metabolic profiles between the four groups. At the same time, to ensure the validity and accuracy of the OPLS-DA data analysis model, it is necessary to carry out overfitting verification. The results (Fig. S2c, d) show that after 200 cross validations, the model had no overfitting phenomenon. To analyze the effects of CRS on the metabolic characteristics of HF mice, further analysis was undertaken for the HF and HF + CRS groups, the PCA (Fig. S3a, b) and OPLS-DA (Fig. 5c, d) revealed an obvious separation between the HF and HF + CRS groups. Moreover, after 200 permutation tests, the results show that the model is reliable (Fig. S3c, d). We eventually found 119 differential metabolites (Table S2). These differential metabolites were subjected to heatmap clustering analysis, as shown in Fig. 5e, these differential metabolites can distinguish the two groups. The pathway enrichment analysis of the differential metabolites revealed these following pathways were significantly perturbed in liver tissue: betaine metabolism; methionine metabolism; pyruvaldehyde degradation; pantothenate and CoA biosynthesis; purine metabolism (Fig. 5f). We then performed analysis with IPA and found some potential key targets associated with differential metabolites, such as, MAPK, AKT, ERK, AMPK, INSR, etc. (Fig. 5g).

3.5 CRS increased betaine levels in liver tissue

Through pathway enrichment analysis, we recognized that the most influential is betaine metabolism. Betaine is an alkaloid with the chemical name of N,N,N-trimethylglycine, the chemical structure (Fig. 6a). Many studies have shown that betaine has therapeutic effects on liver injury. In our study, compared to the HF group, betaine levels were remarkedly increased in the HF + CRS group (Fig. 6b). We purchased

betaine standards as controls, the two metabolites could be further verified according to the retention time and the fragment ions (Fig. 6c, d). The secondary mass spectrometry of these two metabolites is shown in Fig. 7e and f. This provides evidence to identify the authenticity of betaine.

3.6 CRS regulated the INSR/PI3K/AKT/AMPK signaling pathway in HF mice

Combining the results of literature research and metabolomics IPA analysis, we proposed a hypothesis that CRS regulates the INSR/PI3K/AKT/AMPK signaling pathway through upregulation of betaine, thereby alleviate liver injury and HF (Fig. 7a). We then examined the liver tissue protein levels and mRNA expression of INSR, PI3K, AKT, and AMPK. The results showed that these protein levels and gene expression were significantly decreased in the HF group compared to the control and CRS groups and increased in the HF + CRS group compared to the HF group (Fig. 7b-d).

The immunofluorescence (Fig. 8a, b) results of p-AMPK in mouse liver tissue were also consistent with the previous. AMPK is a major regulator of lipid metabolism, and we further examined serum triglyceride (TC) and total cholesterol (TG) levels (Fig. 8c, d), which showed that although there was no statistical difference in triglyceride, total cholesterol expression increased in the HF group and decreased in the HF + CRS group. In conclusion, our results indicated that CRS might ameliorate HF through upregulation of the INSR/PI3K/AKT/AMPK pathway.

4 Discussion

In our study, we established a CRS-involved HF mice model. We noticed that CRS was able to improve liver function and HF caused by CCl_4. Metabolomics analysis showed that CRS altered the metabolic profile of CCl_4-induced HF in mice, where the most significantly altered pathways were betaine metabolism. Betaine is an important nutrient that is synthesized through the choline metabolic pathway and is an endogenous metabolite[19]. In recent years, a large amount of literature has reported that betaine has good preventive and therapeutic effects on a variety of liver diseases, in addition to maintaining normal physiological functions[20–24]. It is worth mentioning that a number of studies have shown that betaine has significant antifibrotic effects on CCl_4-induced liver fibrosis in vitro and in vivo[25–27].Our results showed that CRS increased betaine levels in liver tissue of mice with HF and that there was no significant difference in betaine levels between the normal and CRS groups (Fig. S4). Combining the results of IPA analysis and the literature on betaine treatment of HF, we hypothesize that CRS attenuates CCl_4-induced HF by upregulating the INSR/PI3K/AKT/AMPK pathway through the upregulation of betaine content in liver tissue. This conjecture was confirmed in the subsequent experiments.

Liver diseases are often accompanied by insulin resistance[28–30], when insulin resistance occurs insulin receptor levels in the body are decreased and the ability of insulin to catabolize lipids is diminished, leading to an increase in free fatty acids in the serum, which leads to disorders of lipid metabolism[31–32],

which is consistent with our study in which insulin receptor levels were downregulated and TC levels were increased in liver fibrosis mice, whereas in liver fibrosis mice given CRS we observed upregulation of insulin receptor levels and downregulation of total cholesterol levels.

AMPK is an important molecule in maintaining energy metabolism homeostasis. AMPK activity is increased by 2–3 orders of magnitude by phosphorylation of Thr172 on the α-subunit[33–34]. A close relationship between AMPK and liver fibrosis has been established by clinical studies. It was found that 28 patients with advanced fibrosis/cirrhosis had lower AMPK activity compared to healthy individuals[35]. Some research were demonstrated that activation of AMPK inhibited the expression of TGF-β, tissue inhibitor of metalloproteinase I, collagen and α-SMA, all of which are important factors in promoting liver fibrosis in mice with carbon tetrachloride-induced HF[36–38]. This is consistent with the results of our study. In our study, we found a decrease in p-AMPK levels in CCl_4-induced HF mice and an increase in p-AMPK in HF mice given CRS.

Feelings of stress are familiar to all of us, an encounter with a stressful challenge activates simultaneously the sympathetic nervous system and the hypothalamus-pituitary-adrenal axis[39–40], and thereby provoke the releasing of glucocorticoid corticosterone in rodents and cortisol in humans and adrenal hormones, which are the most important regulatory hormone of the human stress response[41–42]. In the field of neuroscience, the term "stress" has a negative connotation because of its potential to trigger or exacerbate psychopathology. However, in the face of stress, the more common response to stress is resilience, suggesting that resilience is the rule and stress-related pathology the exception[43]. In fact, the physiological stress response has been selected as an important survival response throughout evolution[44–45], stress adaptive response is considered to be the result of compensatory biological processes to restore homeostasis perturbed by stressors. There is accumulating evidence that most stress effects on health are bidirectional, proper stress can enhance memory and learning and improve cognitive function[46–50]. We simulate stress with CRS, which is a milder form of stress. In studies of the relationship between stress and HF, it has also been shown that CRS can reduce HF[12–14], these also provide support for our study.

In our study, behavioral experiments showed that CRS causes normal mice to perform negative behaviors but did not worsen the depression-like behavior of HF mice, and even attenuated the lack of pleasure in HF mice. It is indicating that CRS might be an appropriate stressor for mice with HF. The nature of the stress response is to restore homeostasis in vivo, and chronic restraint stress causes significant changes in the metabolic profile of HF mice, and these changes attenuate the symptoms of HF.

5 Conclusion

Our study, for the first time, demonstrated that CRS alleviates CCl_4-induced liver fibrosis in mice via upregulation of the INSR/PI3K/AKT/AMPK pathway. Moreover, proper stress might serve as a novel therapeutic strategy for HF.

Abbreviations

α-SMA, alpha smooth muscle actin

Acta2, alpha smooth muscle actina

AKT, threonine Kinase

Akt1, threonine Kinase 1

ALP, alkaline phosphatase

ALT, alanine transaminase

AMPK, adenosine 5’-monophosphate (AMP)-activated protein kinase

AST, aspartate aminotransferase

CRS, chronic restraint stress

ECM, extracellular matrix

FST, forced swimming test

HF, hepatic fibrosis

HSCs, hepatic stellate cells

IPA, ingenuity Pathway Analysis

INSR, insulin receptor

Insr, insulin receptor

OFT, open field test

OPLS-DA, orthogonal partial least squares discriminate analysis

PCA, principal component analysis

PI3K, phosphoinositide 3-kinase

Pi3kr1, phosphoinositide-3-kinase regulatory subunit 1

Prkaa1, protein Kinase AMP-Activated Catalytic Subunit Alpha 1

QC, quality control

SPT, sucrose preference test

STD, standard deviation

TC, riglyceride

TG, total cholesterol

TST, tail suspension test

Declarations

Acknowledgments and Funding Information

This study was supported in part by the National Natural Science Foundation of China (82104687, 82274226, 82074219), the Key Laboratory of Guangdong Drug Administration (2021ZDB03), the Key-Area Research and Development Program of Guangdong Province (2020B1111100004), and the 2020 Guangdong Provincial Science and Technology Innovation Strategy Special Fund (Guangdong-Hong Kong-Macau Joint Lab) (2020B1212030006).

Competing Interests

No competing financial interests exist.

Author Contributions

Shanshan Zhang: Performing the experiments, Data curation, Writing original draft. Binjie Liu: Validation, Investigation. Lan Huang: Experimental assistance. Rong Zhang: Writing-Review & Editing, Supervision. Lin An: Writing - Review & Editing, Methodology, Funding acquisition. Zhongqiu Liu: Conceptualization, Funding acquisition, Writing-Review & Editing.

Corresponding author

Correspondence to Zhongqiu Liu or Lin An.

Data availability

All data analyses during this study are included in this published article, and all data generated during the study are available from the corresponding author on request.

Ethics approval

The animal experiments were approved by the Institutional Animal Care and Use Committee of Guangzhou University of Traditional Chinese Medicine (reference No. 20211102).

References

1. Roehlen N, Crouchet E, Baumert TF (2020) Liver Fibrosis: Mechanistic Concepts and Therapeutic Perspectives. Cells 9(4):875. https://doi.org/10.3390/cells9040875
2. Parola M, Pinzani M (2019) Liver fibrosis: Pathophysiology, pathogenetic targets and clinical issues. Mol Aspects Med 65:37–55. https://doi.org/10.1016/j.mam.2018.09.002
3. Ren L, Qi K, Zhang L, Bai Z, Ren C, Xu X, Zhang Z, Li X (2019) Glutathione Might Attenuate Cadmium-Induced Liver Oxidative Stress and Hepatic Stellate Cell Activation. Biol Trace Elem Res 191(2):443–452. https://doi.org/10.1007/s12011-019-1641-x
4. Kisseleva T, Brenner D (2021) Molecular and cellular mechanisms of liver fibrosis and its regression. Nat Rev Gastroenterol Hepatol 18(3):151–166. https://doi.org/10.1038/s41575-020-00372-7
5. Ginès P, Krag A, Abraldes JG, Solà E, Fabrellas N, Kamath PS (2021) Liver cirrhosis. Lancet (London England) 398(10308):1359–1376. https://doi.org/10.1016/S0140-6736(21)01374-X
6. Friedman SL, Pinzani M (2022) Hepatic fibrosis 2022: Unmet needs and a blueprint for the future. Hepatology 75(2):473–488. https://doi.org/10.1002/hep.32285
7. Guo H, Zheng L, Xu H, Pang Q, Ren Z, Gao Y, Wang T (2022) Neurobiological Links between Stress, Brain Injury, and Disease. Oxidative medicine and cellular longevity, 2022, 8111022. https://doi.org/10.1155/2022/8111022
8. Osborne MT, Shin LM, Mehta NN, Pitman RK, Fayad ZA, Tawakol A (2020) Disentangling the Links Between Psychosocial Stress and Cardiovascular Disease. Circ Cardiovasc Imaging 13(8):e010931. https://doi.org/10.1161/CIRCIMAGING.120.010931
9. Margolis KG, Cryan JF, Mayer EA (2021) The Microbiota-Gut-Brain Axis: From Motility to Mood. Gastroenterology 160(5):1486–1501. https://doi.org/10.1053/j.gastro.2020.10.066
10. Rohleder N (2019) Stress and inflammation - The need to address the gap in the transition between acute and chronic stress effects. Psychoneuroendocrinology 105:164–171. https://doi.org/10.1016/j.psyneuen.2019.02.021
11. Ceci FM, Ferraguti G, Petrella C, Greco A, Tirassa P, Iannitelli A, Ralli M, Vitali M, Ceccanti M, Chaldakov GN, Versacci P, Fiore M (2021) Nerve Growth Factor, Stress and Diseases. Curr Med Chem 28(15):2943–2959. https://doi.org/10.2174/0929867327999200818111654
12. Yang X, Han ZP, Zhang SS, Zhu PX, Hao C, Fan TT, Yang Y, Li L, Shi YF, Wei LX (2014) Chronic restraint stress decreases the repair potential from mesenchymal stem cells on liver injury by inhibiting TGF-β1 generation. Cell Death Dis 5(6):e1308. https://doi.org/10.1038/cddis.2014.257
13. Li M, Sun Q, Li S, Zhai Y, Wang J, Chen B, Lu J (2016) Chronic restraint stress reduces carbon tetrachloride-induced liver fibrosis. Experimental and therapeutic medicine 11(6):2147–2152. https://doi.org/10.3892/etm.2016.3205
14. Takada S, Matsubara T, Fujii H, Sato-Matsubara M, Daikoku A, Odagiri N, Amano-Teranishi Y, Kawada N, Ikeda K (2021) Stress can attenuate hepatic lipid accumulation via elevation of hepatic β-

muricholic acid levels in mice with nonalcoholic steatohepatitis. Laboratory investigation. J Tech methods Pathol 101(2):193–203. https://doi.org/10.1038/s41374-020-00509-x

15. Corona-Pérez A, Díaz-Muñoz M, Cuevas-Romero E, Luna-Moreno D, Valente-Godínez H, Vázquez-Martínez O, Martínez-Gómez M, Rodríguez-Antolín J, Nicolás-Toledo L (2017) Interactive effects of chronic stress and a high-sucrose diet on nonalcoholic fatty liver in young adult male rats. Stress 20(6):608–617. https://doi.org/10.1080/10253890.2017.1381840
16. Cheng F, Ma C, Wang X, Zhai C, Wang G, Xu X, Mu J, Li C, Wang Z, Zhang X, Yue W, Du X, Lian Y, Zhu W, Yin X, Wei Z, Song W, Wang Q (2017) Effect of traditional Chinese medicine formula Sinisan on chronic restraint stress-induced nonalcoholic fatty liver disease: a rat study. BMC Complement Altern Med 17(1):203. https://doi.org/10.1186/s12906-017-1707-2
17. Ramos-Vara JA Principles and Methods of Immunohistochemistry. Methods in molecular biology (, Clifton NJ (2017) 1641, 115–128. https://doi.org/10.1007/978-1-4939-7172-5_5
18. Zheng J, Zheng Y, Li W, Zhi J, Huang X, Zhu W, Liu Z, Gong L (2022) Combined metabolomics with transcriptomics reveals potential plasma biomarkers correlated with non-small-cell lung cancer proliferation through the Akt pathway. Int J Clin Chem 530:66–73. https://doi.org/10.1016/j.cca.2022.02.018. Clinica chimica acta
19. Wang C, Ma C, Gong L, Dai S, Li Y (2021) Preventive and therapeutic role of betaine in liver disease: A review on molecular mechanisms. Eur J Pharmacol 912:174604. https://doi.org/10.1016/j.ejphar.2021.174604
20. Rehman A, Mehta KJ (2022) Betaine in ameliorating alcohol-induced hepatic steatosis. Eur J Nutr 61(3):1167–1176. https://doi.org/10.1007/s00394-021-02738-2
21. Chen W, Zhang X, Xu M, Jiang L, Zhou M, Liu W, Chen Z, Wang Y, Zou Q, Wang L (2021) Betaine prevented high-fat diet-induced NAFLD by regulating the FGF10/AMPK signaling pathway in ApoE-/- mice. Eur J Nutr 60(3):1655–1668. https://doi.org/10.1007/s00394-020-02362-6
22. Hagar H, Husain S, Fadda LM, Attia NM, Attia MMA, Ali HM (2019) Inhibition of NF-κB and the oxidative stress -dependent caspase-3 apoptotic pathway by betaine supplementation attenuates hepatic injury mediated by cisplatin in rats. Pharmacol Rep 71(6):1025–1033. https://doi.org/10.1016/j.pharep.2019.06.003
23. Khodayar MJ, Kalantari H, Khorsandi L, Rashno M, Zeidooni L (2020) Upregulation of Nrf2-related cytoprotective genes expression by acetaminophen-induced acute hepatotoxicity in mice and the protective role of betaine. Hum Exp Toxicol 39(7):948–959. https://doi.org/10.1177/0960327120905962
24. Veskovic M, Mladenovic D, Milenkovic M, Tosic J, Borozan S, Gopcevic K, Labudovic-Borovic M, Dragutinovic V, Vucevic D, Jorgacevic B, Isakovic A, Trajkovic V, Radosavljevic T (2019) Betaine modulates oxidative stress, inflammation, apoptosis, autophagy, and Akt/mTOR signaling in methionine-choline deficiency-induced fatty liver disease. Eur J Pharmacol 848:39–48. https://doi.org/10.1016/j.ejphar.2019.01.043

25. Bingül İ, Başaran-Küçükgergin C, Aydın AF, Çoban J, Doğan-Ekici I, Doğru-Abbasoğlu S, Uysal M (2016) Betaine treatment decreased oxidative stress, inflammation, and stellate cell activation in rats with alcoholic liver fibrosis. Environ Toxicol Pharmacol 45:170–178. https://doi.org/10.1016/j.etap.2016.05.033
26. Tsai MT, Chen CY, Pan YH, Wang SH, Mersmann HJ, Ding ST (2015) Alleviation of Carbon-Tetrachloride-Induced Liver Injury and Fibrosis by Betaine Supplementation in Chickens. Evidence-based complementary and alternative medicine: eCAM, 2015, 725379. https://doi.org/10.1155/2015/725379
27. Quesada-Vázquez S, Colom-Pellicer M, Navarro-Masip È, Aragonès G, Del Bas JM, Caimari A, Escoté X (2021) Supplementation with a Specific Combination of Metabolic Cofactors Ameliorates Non-Alcoholic Fatty Liver Disease, Hepatic Fibrosis, and Insulin Resistance in Mice. Nutrients 13(10):3532. https://doi.org/10.3390/nu13103532
28. Dai Y, Hao P, Sun Z, Guo Z, Xu H, Xue L, Song H, Li Y, Li S, Gao M, Si T, Zhang Y, Qi Y (2021) Liver knockout YAP gene improved insulin resistance-induced hepatic fibrosis. J Endocrinol 249(2):149–161. https://doi.org/10.1530/JOE-20-0561
29. Eshaghian A, Khodarahmi A, Safari F, Binesh F, Moradi A (2018) Curcumin attenuates hepatic fibrosis and insulin resistance induced by bile duct ligation in rats. Br J Nutr 120(4):393–403. https://doi.org/10.1017/S0007114518001095
30. Fujii H, Kawada N, Japan Study Group Of Nafld Jsg-Nafld (2020) The Role of Insulin Resistance and Diabetes in Nonalcoholic Fatty Liver Disease. Int J Mol Sci 21(11):3863. https://doi.org/10.3390/ijms21113863
31. Horn CL, Morales AL, Savard C, Farrell GC, Ioannou GN (2022) Role of Cholesterol-Associated Steatohepatitis in the Development of NASH. Hepatol Commun 6(1):12–35. https://doi.org/10.1002/hep4.1801
32. Gaggini M, Carli F, Rosso C, Younes R, D'Aurizio R, Bugianesi E, Gastaldelli A (2019) Altered Metabolic Profile and Adipocyte Insulin Resistance Mark Severe Liver Fibrosis in Patients with Chronic Liver Disease. Int J Mol Sci 20(24):6333. https://doi.org/10.3390/ijms20246333
33. Yan Y, Zhou XE, Xu HE, Melcher K (2018) Structure and Physiological Regulation of AMPK. Int J Mol Sci 19(11):3534. https://doi.org/10.3390/ijms19113534
34. Zhang CS, Jiang B, Li M, Zhu M, Peng Y, Zhang YL, Wu YQ, Li TY, Liang Y, Lu Z, Lian G, Liu Q, Guo H, Yin Z, Ye Z, Han J, Wu JW, Yin H, Lin SY, Lin SC (2014) The lysosomal v-ATPase-Ragulator complex is a common activator for AMPK and mTORC1, acting as a switch between catabolism and anabolism. Cell Metabol 20(3):526–540. https://doi.org/10.1016/j.cmet.2014.06.014
35. Ramezani-Moghadam M, Wang J, Ho V, Iseli TJ, Alzahrani B, Xu A, Van der Poorten D, Qiao L, George J, Hebbard L (2015) Adiponectin reduces hepatic stellate cell migration by promoting tissue inhibitor of metalloproteinase-1 (TIMP-1) secretion. J Biol Chem 290(9):5533–5542. https://doi.org/10.1074/jbc.M114.598011

36. Liu G, Cui Z, Gao X, Liu H, Wang L, Gong J, Wang A, Zhang J, Ma Q, Huang Y, Piao G, Yuan H (2021) Corosolic acid ameliorates non-alcoholic steatohepatitis induced by high-fat diet and carbon tetrachloride by regulating TGF-β1/Smad2, NF-κB, and AMPK signaling pathways. Phytother Res 35(9):5214–5226. https://doi.org/10.1002/ptr.7195
37. Shin MR, Lee JA, Kim M, Lee S, Oh M, Moon J, Nam JW, Choi H, Mun YJ, Roh SS (2021) Gardeniae Fructus Attenuates Thioacetamide-Induced Liver Fibrosis in Mice via Both AMPK/SIRT1/NF-κB Pathway and Nrf2 Signaling. Antioxid (Basel Switzerland) 10(11):1837. https://doi.org/10.3390/antiox10111837
38. Wu J, Xue X, Fan G, Gu Y, Zhou F, Zheng Q, Liu R, Li Y, Ma B, Li S, Huang G, Ma L, Li X (2021) Ferulic Acid Ameliorates Hepatic Inflammation and Fibrotic Liver Injury by Inhibiting PTP1B Activity and Subsequent Promoting AMPK Phosphorylation. Front Pharmacol 12:754976. https://doi.org/10.3389/fphar.2021.754976
39. Russell AL, Tasker JG, Lucion AB, Fiedler J, Munhoz CD, Wu TJ, Deak T (2018) Factors promoting vulnerability to dysregulated stress reactivity and stress-related disease. J Neuroendocrinol 30(10):e12641. https://doi.org/10.1111/jne.12641
40. Zänkert S, Bellingrath S, Wüst S, Kudielka BM (2019) HPA axis responses to psychological challenge linking stress and disease: What do we know on sources of intra- and interindividual variability? Psychoneuroendocrinology 105:86–97. https://doi.org/10.1016/j.psyneuen.2018.10.027
41. Kageyama K, Iwasaki Y, Daimon M (2021) Hypothalamic Regulation of Corticotropin-Releasing Factor under Stress and Stress Resilience. Int J Mol Sci 22(22):12242. https://doi.org/10.3390/ijms222212242
42. Herman JP (2022) The neuroendocrinology of stress: Glucocorticoid signaling mechanisms. Psychoneuroendocrinology 137:105641. https://doi.org/10.1016/j.psyneuen.2021.105641
43. Richter-Levin G, Sandi C (2021) Title: "Labels Matter: Is it stress or is it Trauma?". Translational psychiatry 11(1):385. https://doi.org/10.1038/s41398-021-01514-4
44. Ellis BJ, Del Giudice M (2019) Developmental Adaptation to Stress: An Evolutionary Perspective. Ann Rev Psychol 70:111–139. https://doi.org/10.1146/annurev-psych-122216-011732
45. Deussing JM, Chen A (2018) The Corticotropin-Releasing Factor Family: Physiology of the Stress Response. Physiol Rev 98(4):2225–2286. https://doi.org/10.1152/physrev.00042.2017
46. Goldfarb EV (2019) Enhancing memory with stress: Progress, challenges, and opportunities. Brain Cogn 133:94–105. https://doi.org/10.1016/j.bandc.2018.11.009
47. Plieger T, Reuter M (2020) Stress & executive functioning: A review considering moderating factors. Neurobiol Learn Mem 173:107254. https://doi.org/10.1016/j.nlm.2020.107254
48. Schwabe L, Joëls M, Roozendaal B, Wolf OT, Oitzl MS (2012) Stress effects on memory: an update and integration. Neurosci Biobehav Rev 36(7):1740–1749. https://doi.org/10.1016/j.neubiorev.2011.07.002
49. Shields GS, Sazma MA, McCullough AM, Yonelinas AP (2017) The effects of acute stress on episodic memory: A meta-analysis and integrative review. Psychol Bull 143(6):636–675.

https://doi.org/10.1037/bul0000100

50. Sazma MA, McCullough AM, Shields GS, Yonelinas AP (2019) Using acute stress to improve episodic memory: The critical role of contextual binding. Neurobiol Learn Mem 158:1–8. https://doi.org/10.1016/j.nlm.2019.01.001

Figures

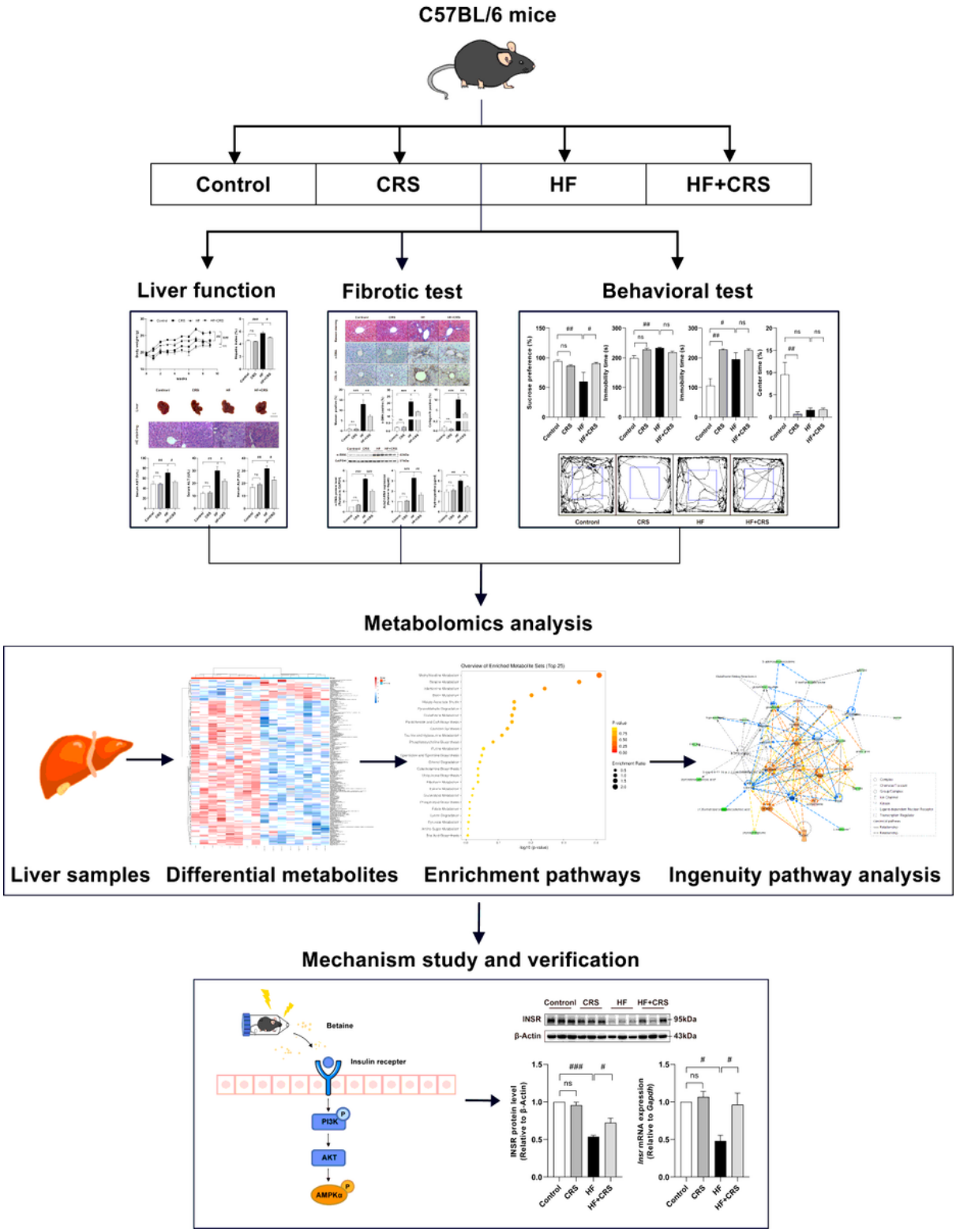

Figure 1

Flowchart illustrating the experimental design of the study

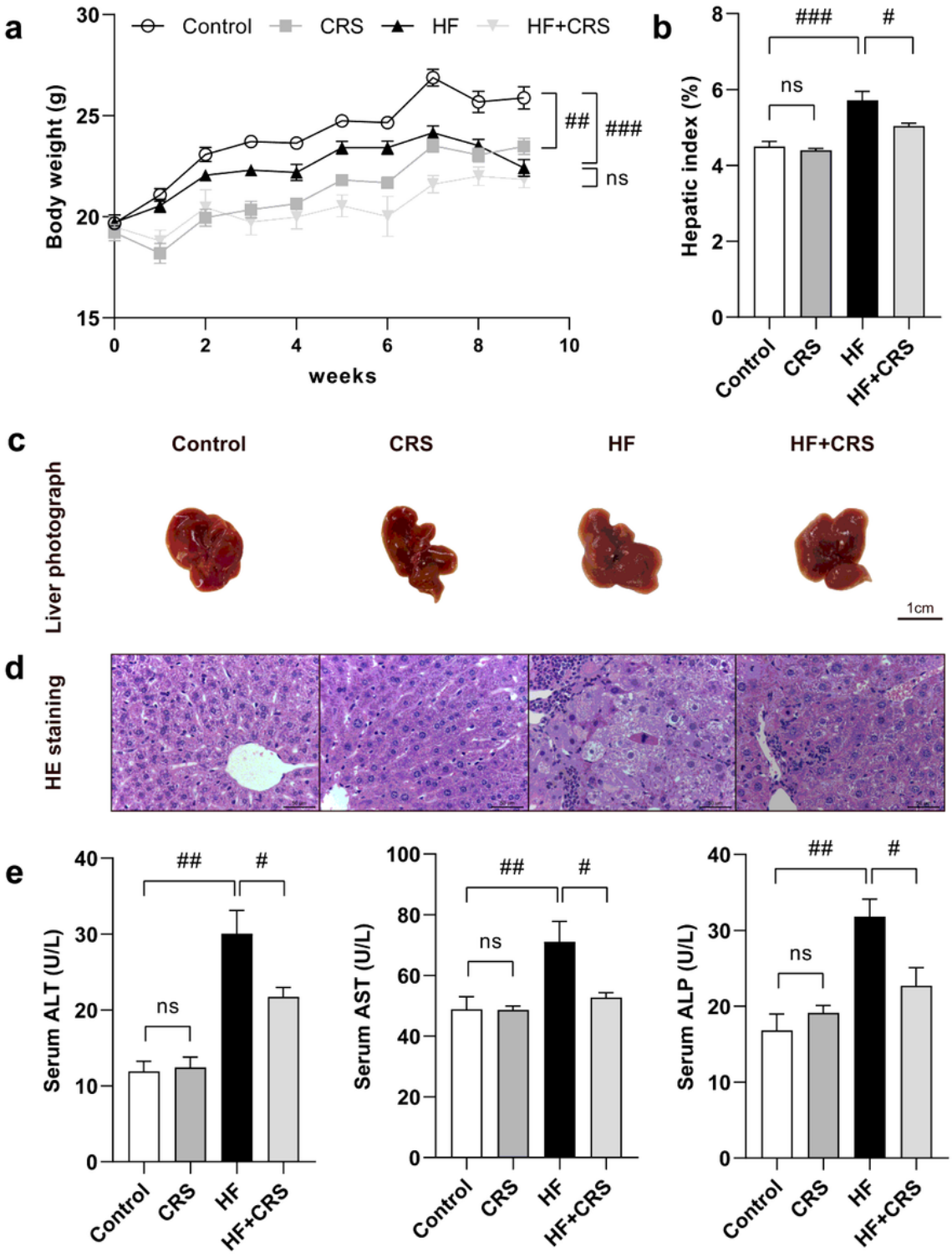

Figure 2

CRS attenuates CCl_4-induced liver injury. (a) The changes of body weight during the experimental course (n = 5). (b) Liver coefficient after 9 weeks (n = 5). (c) Live photographs of mice livers. (d) Histopathological examination of liver sections stained with H&E (400×). (e) Determination of the serum ALT, AST and ALP with assay kits (n = 5). Data represent mean ± *SEM*, $^{\#}p < 0.05$, $^{\#\#}p < 0.01$ versus the indicated group

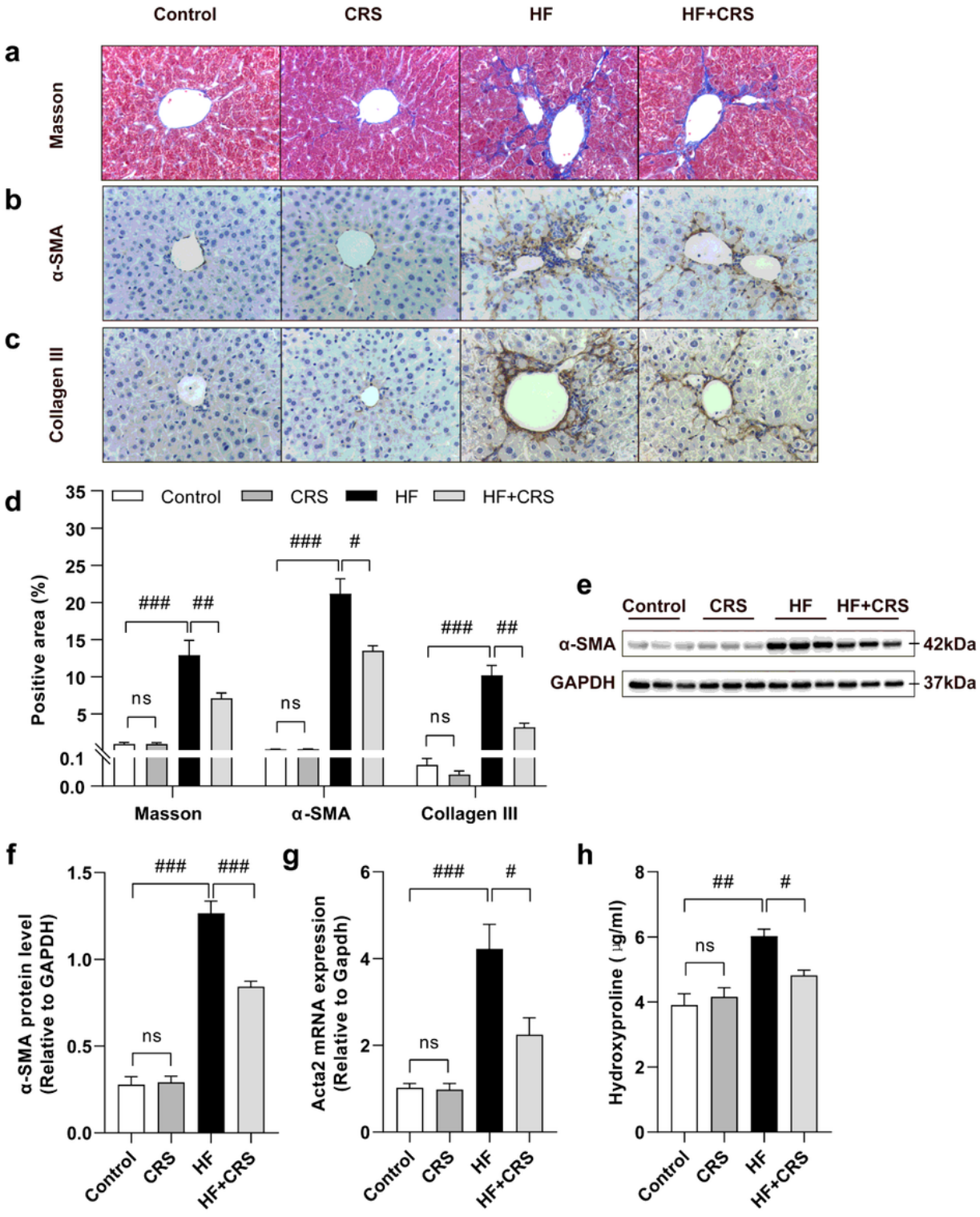

Figure 3

CRS alleviates CCl_4-induced liver fibrosis in mice. (a) Representative images of Masson staining (400x). (b-c) Immunohistochemical staining of α-SMA and collagen-III of liver sections (400x). (d) Quantitative results of Masson staining, α-SMA and collagen-III immunohistochemical staining. (e) Western blot analysis of α-SMA protein level (n = 5). (f) Quantitative results of western blot analysis of α-SMA. (g) Real-time PCR analysis of α-SMA mRNA expression (n = 4). (h) Serum level of hydroxyproline was tested by biochemical kit (n = 5). Data represent mean ± *SEM*, $^{\#}p < 0.05$, $^{\#\#}p < 0.01$, $^{\#\#\#}p < 0.001$ versus the indicated group

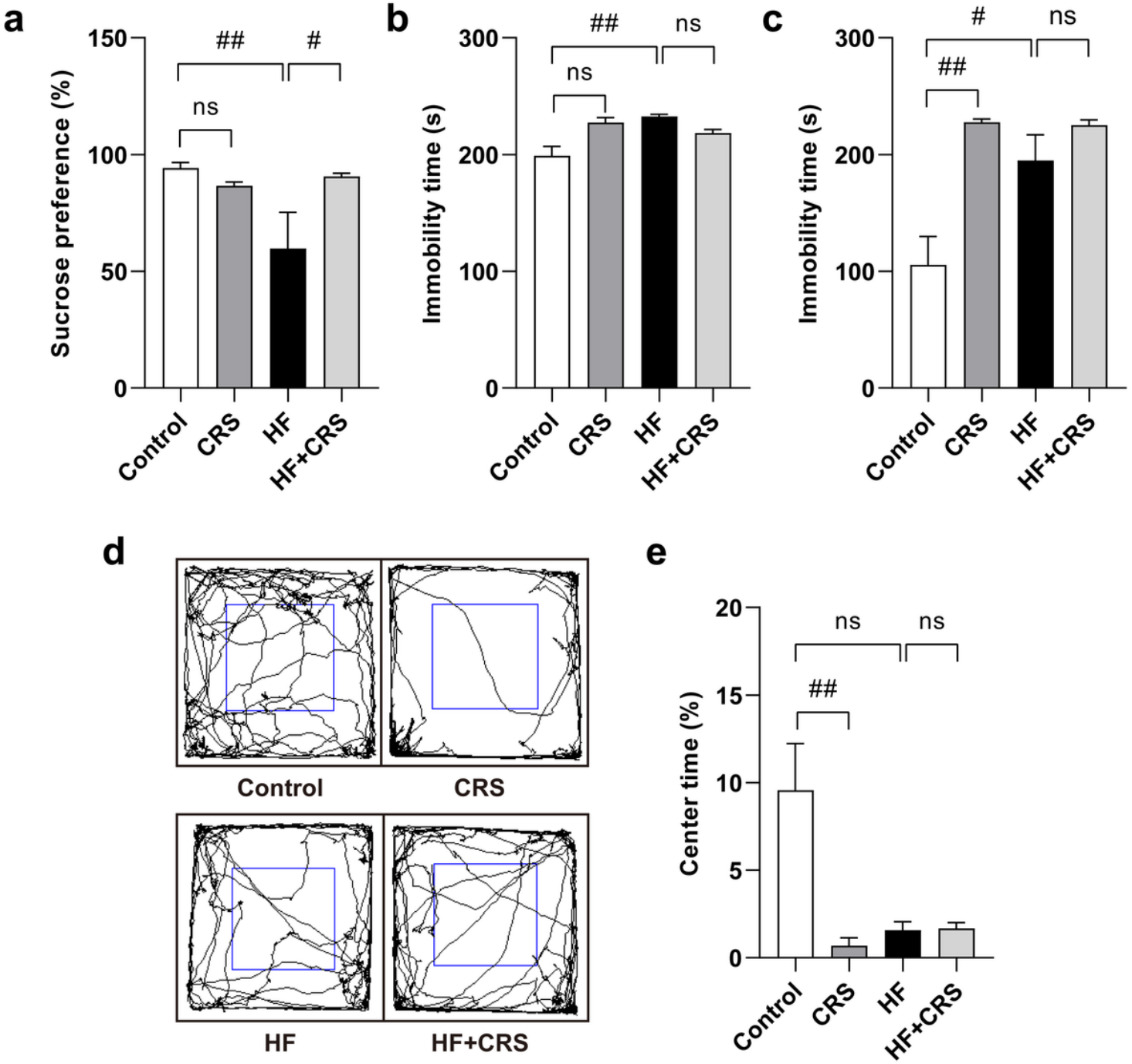

Figure 4

CCl_4-induced liver fibrosis can cause depression-like behavior. (a) Results of sucrose preference experiments (n = 5). (b) Immobility time of tail suspension test (n = 5). (c) Immobility time of forced swimming test (n = 5). (d) Trajectory diagram of open field test. (e) The center time percentage of open field test (n = 5). Data represent mean ± *SEM.*, $^{\#}p < 0.05$, $^{\#\#}p < 0.01$ versus the indicated group

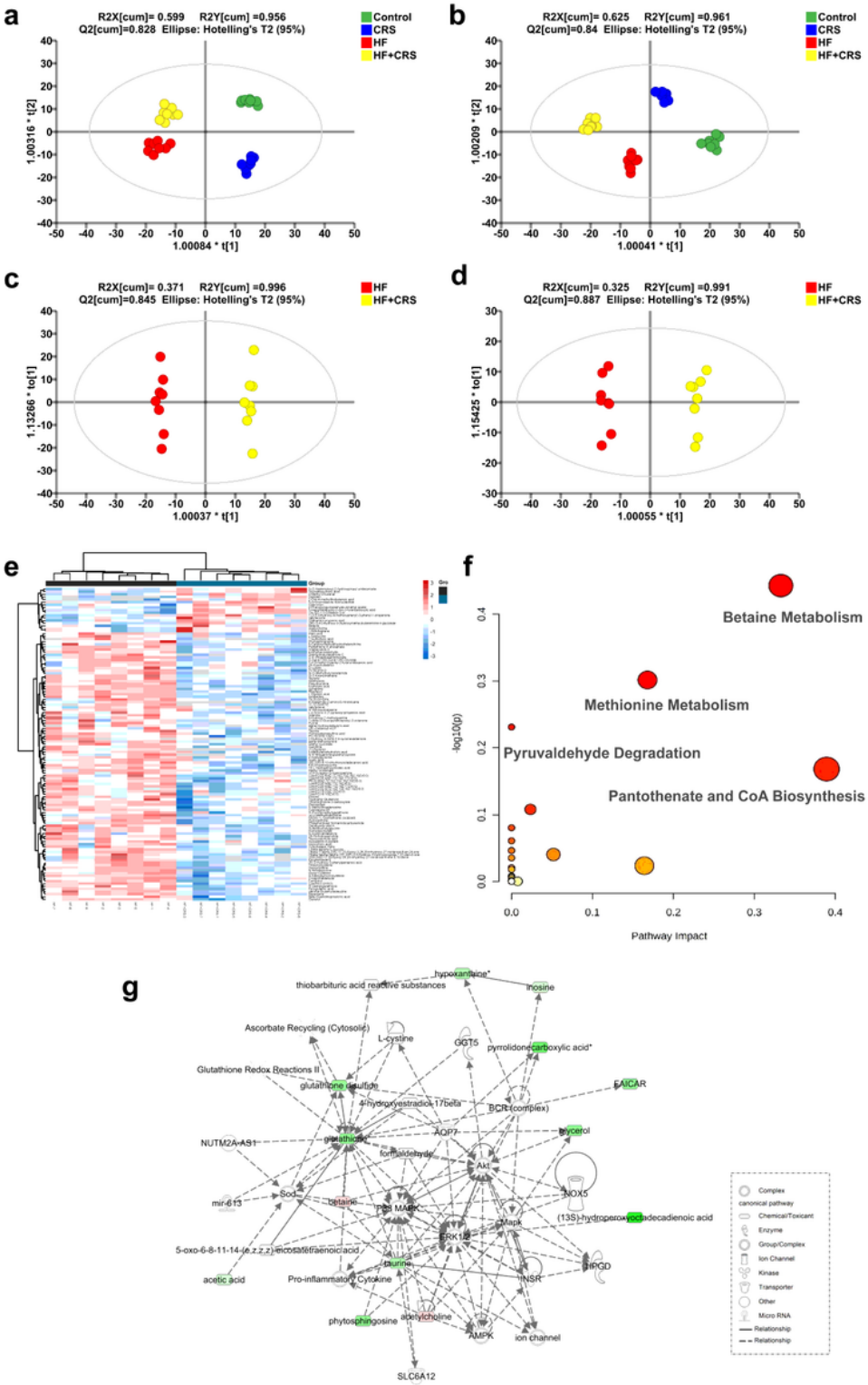

Figure 5

Metabolomic analysis of liver tissue. (a-b) OPLS-DA scatter plot of metabolic profiles in positive (left panel) and negative (right panel) ion mode of four groups (*n* = 8). (c-d) OPLS-DA scatter plot of metabolic profiles in positive (left panel) and negative (right panel) ion mode between the HF and HF+CRS treatment (*n* = 8). (e) The heatmap analysis of 119 differential metabolites. (f) Differential metabolite pathways analysis. (g) Ingenuity Pathway Analysis of differential metabolites

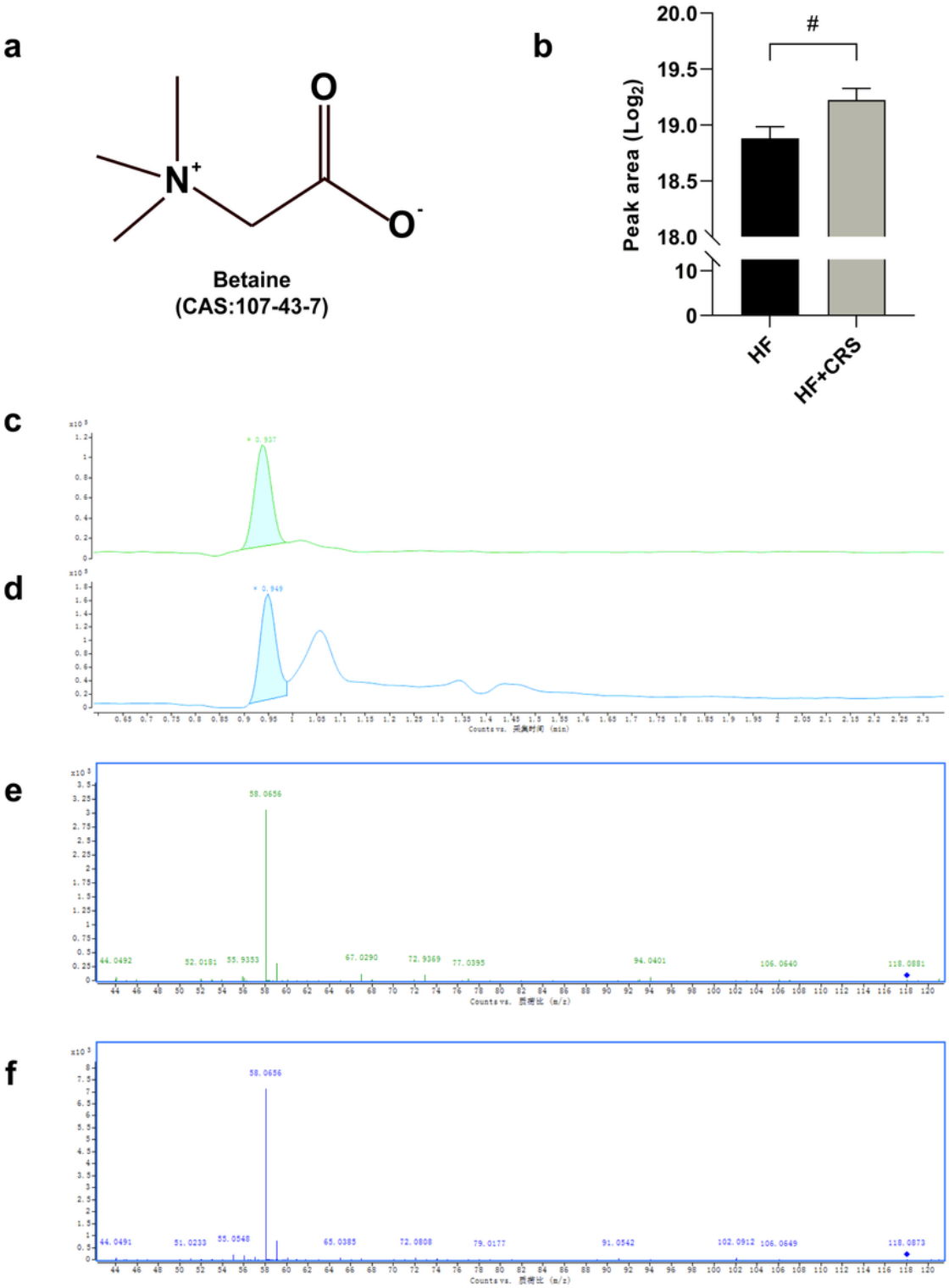

Figure 6

The secondary mass spectrogram of the betaine (a) Chemical structure formula of betaine. (b) Quantification of betaine peak area (n = 8). (c-d) The chromatogram of betaine standard (upper panel) and betaine in the sample (lower panel). (e-f) The secondary mass spectrogram of betaine standard (upper panel) and betaine in the sample (lower panel). Data represent mean ± *SEM*, $^{\#}p < 0.05$ versus the indicated group

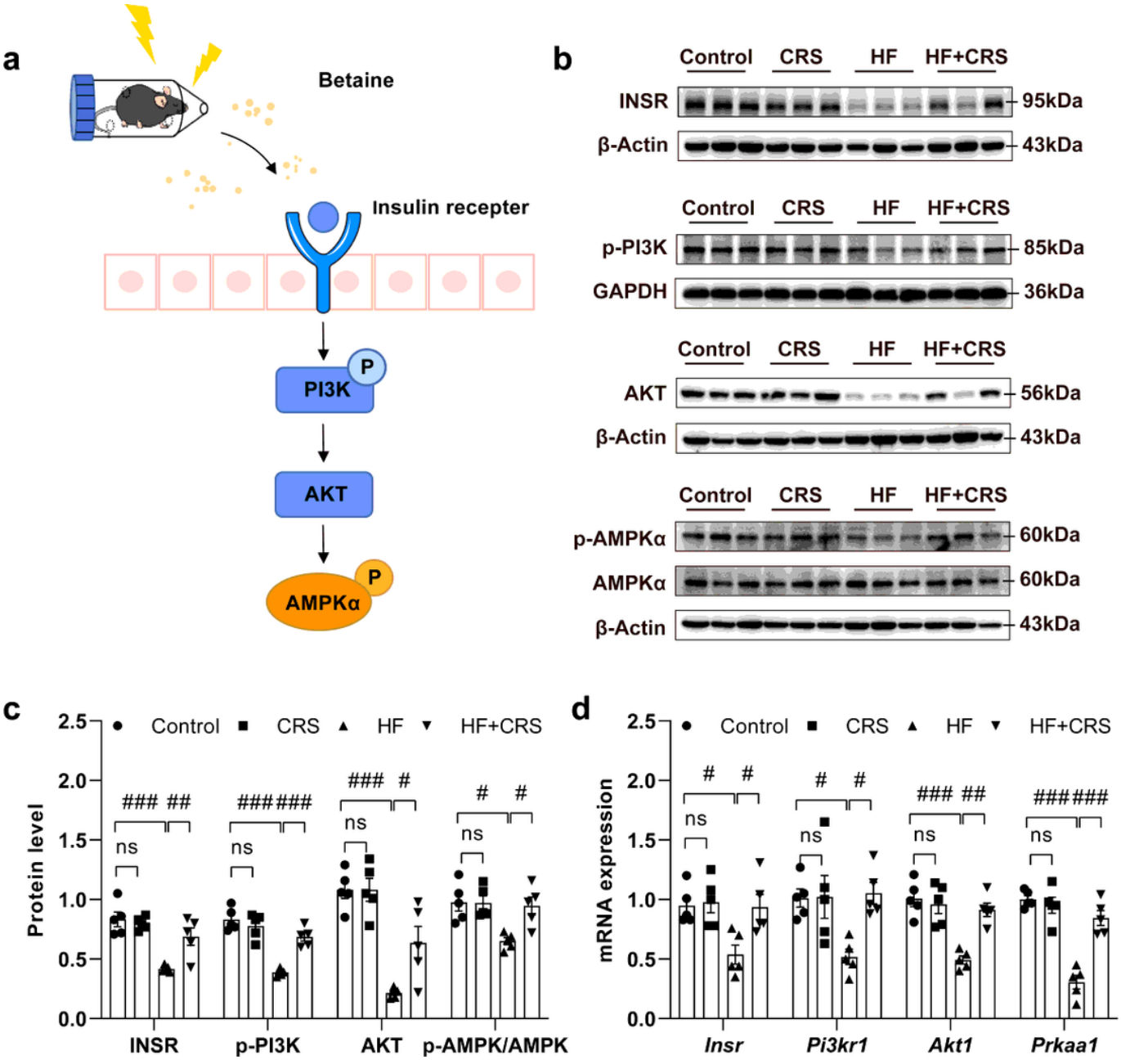

Figure 7

INSR/PI3K/AKT/AMPK signaling pathway were get involved in the regulation of CRS alleviated CCl_4-induced HF in mice. (a) Hypothetical mechanism graph of CRS alleviated CCl_4-induced HF in mice. (b) Representative western blot analysis of INSR, PI3K, AKT and AMPK protein level. (c) The semi-quantitative results of western blot analysis of INSR, PI3K, AKT and AMPK (n = 5). (d)The real-time PCR

analysis of INSR, PI3K, AKT and AMPK mRNA expression ($n = 5$). Data represent mean ± *SEM*, $^{\#}p < 0.05$, $^{\#\#}p < 0.01$, $^{\#\#\#}p < 0.001$ versus the indicated group

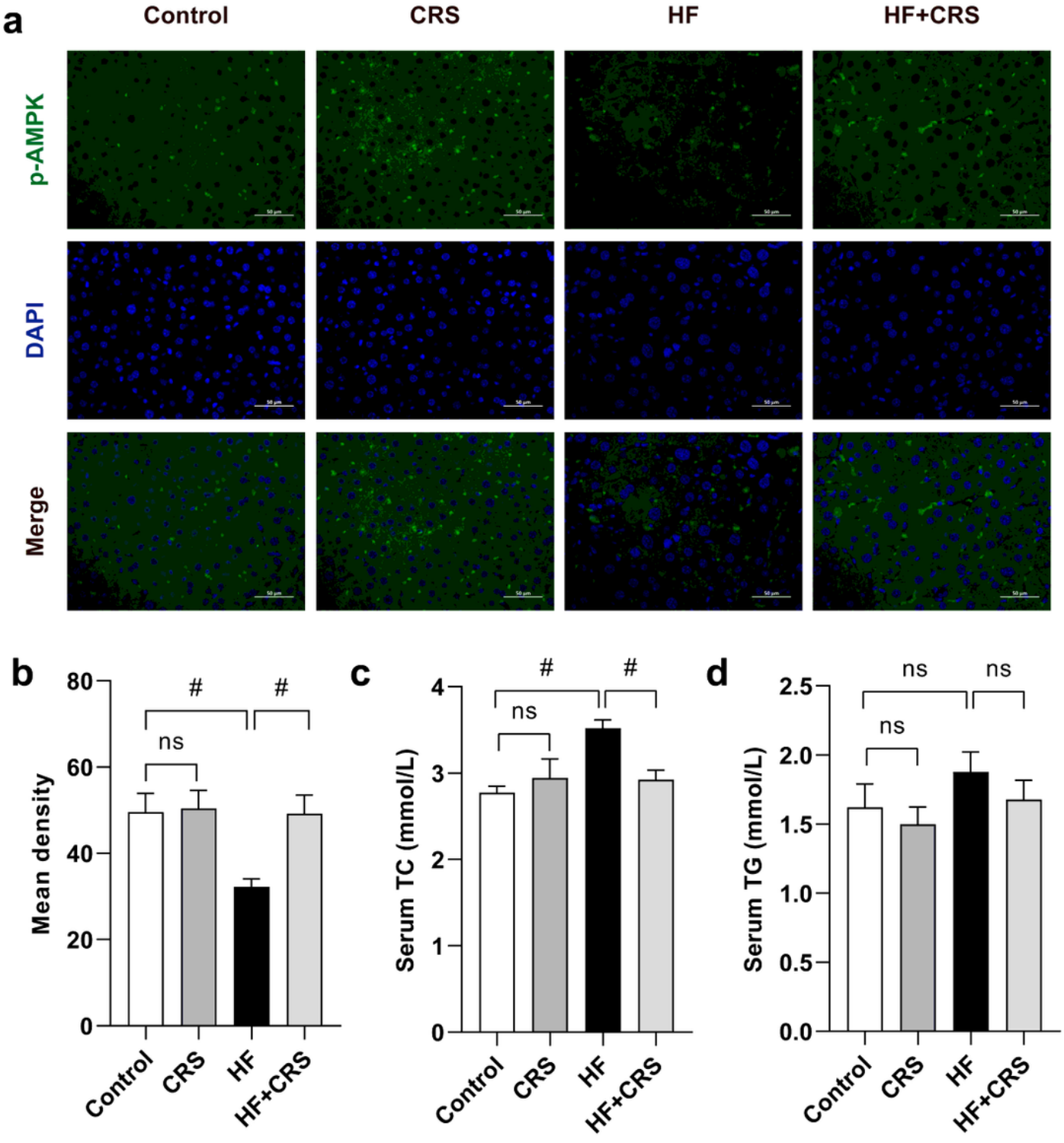

Figure 8

CRS elevated p-AMPK expression in liver tissue of CCl_4-induced HF mice. (a) Immunofluorescence staining of p-AMPK. (b) The quantitative analysis of p-AMPK in immunofluorescence staining. (c) TC

level testing. (d) TG level test. Data represent mean ± *SEM*, $^{\#}p < 0.05$, $^{\#\#}p < 0.01$, $^{\#\#\#}p < 0.001$ versus the indicated group

Supplementary Files

This is a list of supplementary files associated with this preprint. Click to download.

- SupplementaryInformation.pdf